JCAMECH

Vol. 51, No. 2, December 2020, pp 323-331
DOI: 10.22059/jcamech.2019.288693.426

Influence of Magnetic Wire Positions on Free Convection of Fe_3O_4-Water Nanofluid in a Square Enclosure Utilizing with MAC Algorithm

K Venkatadri[a] ∗, A Shobha [b], C Venkata Lakshmi[b], V.Ramachandra Prasad[c], B. Md. Hidayathulla Khan[d]

[a] *Department of Mathematics, SreenivasInstitute of Technology and management sciences, Chittor-517127, India*
[b]*Department of Applied Mathematics, Sri Padmavathi Mahila VisvaVidyalyam, Tirupati 517502, AP, India*
[c]*Department of Mathematics, SAS, Vellore Institute of Technology, Vellore-517112, Indiad*
[d]*Department of Mathematics, Sir Vishveshwaraiah Institute of Science and Technology, Madanapalle-517325, India*

ARTICLE INFO

Article history:
Received: 9 September 2020
Accepted: 18 December 2020

Keywords:
MAC Method
Magnetizable Fluid
Magnetic Sources
Enclosure
Nanofluid

ABSTRACT

The augment of heat transfer and fluid of buoyancy-driven flow of Fe3O4-Water nanofluid in a square cavity under the influence of an external magnetic field is studied numerically. Cold temperature is applied on the side (vertical) walls and high temperature is imposed on the bottom wall while the top wall is kept at thermally insulated. The governing non-dimensional differential equations are solved using Marker and Cell (MAC) Algorithm. The developed MATLAB code is validated with previous literature and it gives good agreement. The effects of Rayleigh number Ra, Prandtl number Pr and Hartmann number Ha on the flow and heat transfer characteristics are analyzed. Results indicate that the temperature gradient is an increasing function of the buoyancy force. The heat transfer characteristics and flow behavior are presented in the form of streamlines and isotherms. The position of magnetic wire is played a vital role in controlling of heat transfer rate.

1. Introduction

Nanotechnology plays an innovative tool for enhancement of heat transfer. Magnetic nanofluids (ferrofluid) are also called smart fluids or functional fluids, which are stable colloidal suspensions of sub-domain magnetic particles (iron, nickel, cobalt, and their oxides such as magnetite) with a particle size of less than20 *nm* dispersed in a base fluid such as water, oil, ethylene glycol, *etc*. The stability of suspension, a monolayer of insoluble surfactant is discussed and reported [1–3]. Magnetic nanofluids are gained much interest in recent years, whereas it has used controlled by external magnetic field (MF) and have received several applications, which includes dynamic sealing, heat dissipation, damping and doping technological materials [4–6]. Most published studies on ferrofluid have focus on enhancing heat transfer by experimental and numerical methods [7–10].

One of the most scientific challenges in the industrial areas is cooling technology. Increasing the rate of cooling by traditional tools (*i.e*. fins and micro channel) has already reached their limits. Nanofluid, an engineered colloidal suspension of nanoparticles in a base fluid, have been applied in several engineering applications, which includes, the photonics, transportation, electronics, and energy supply industries [11–15] due to its enhanced thermal conductivity and convective heat transfer coefficient compared to the base fluid [16–19]. Heat transfer enhancement through nanofluid in a square cavity is studied numerically, the first person Khanafer *et al*. [20]. They also notice that to increase of nanoparticles volume fractions leads to the rate of nanofluid heat transfer is increased. Jang and Choi [21] investigated thermal characteristics in a rectangular enclosure with water based nanofluid. They are conducted numerical analysis of the rectangular enclosure heated from bottom wall; in addition, they are taken 6 *nm* copper and 2 *nm* diamond. Stoian *et al*. [22] study natural convection enhancement through magnetic nanofluid (F_3O_4) by experimentally. Aaiza Gul *et al*. [23] conducted comparison study of MHD mixed convection between water with magnetic (Fe_3O_4) ferric oxides nanoparticles non-magnetic (Al_2O_3) aluminium oxides nanoparticles of vertical channel. Nader *et al*. [24] Carried out natural convection study of non-uniform heating of bottom wall (other walls are isothermal cold walls) of square enclosure with different water based nanofluid. Sinusoidal heating of side wall of enclosure-based study of natural convection of water based nanofluid (Fe_3O_4) with joule heating and constant magnetic field is examined by [25]. They are found that the heat transfer improvement rate by the ferrite nanoparticles with base

* Corresponding author. e-mail: venkatadri.venki@gmail.com

fluid. The influence of inclination on natural convection of water-Based nanofluid in a ***C** shaped enclosure* is study by numerically with constant magnetic field is reported [26]. The similar work is done by Abedini *et al*. [27], this study they are implemented SIMPLE algorithm and studied the natural convection in C-shaped enclosure filled with water based nanofluid (Fe_3O_4) with the influence of baffle and magnetic field. Convective flows and heat transfer analysis in a rectangular enclosure with water –Fe_3O_4 under the affected oval – shaped heat source within the enclose is introduced by Moraveji and Hejazian [28]. They are studied heat transfer characteristics in a water based nanofluid (Fe_3O_4) with different size of oval-shaped heat source.

A ferrofluid acts as a fluid that is influenced by a magnetic wire and externally imposed magnetic fields has been used to control and fluid direct of ferrofluid, due to its numerous applications in science and engineering. Which include, electronic packing, mechanical engineering, thermal engineering, aerospace and bioengineering [29–32]. Sheikholeslami *et al*. [33] examine the impact of external magnetic field on natural convection of water – Fe_3O_4 in an enclosure. Sheikholeslami and Vajravelu [34] performed control volume based finite element method of natural convection of water –Fe_3O_4 in a square enclosure in presence of heat source has constant heat flux on bottom wall and the influence of the variable magnetic source. Sheikholeslami and Ganji [35] simulated the convective flow in an enclosure (shape =1/4 of circle portion) with the impact of variable magnetic field and they are found the effect of radiation becomes stronger for higher buoyancy forces. Sheikholeslami *et al*. [36] analyzed flow and heat transfer in a porous enclosure with same geometry of [35] under the impact of external magnetic field. Combined magnetohydrodynamic and ferrohydrodynamic effects on water – Fe_3O_4 in an enclosure with constant heat flux of inner boundary and constant temperature of out boundary in presence of dipole external magnetic sources has been discussed [37] and the same enclosure with inner circular boundary has constant hot temperature whereas the other walls are isothermal cold temperature with the impact of opposite variable magnetic wires are performed [38]. The flow and heat transfer are examined with the impact of magnetic field and the non-dimensional governing equations are employed by the effect projection scheme in MAC algorithm has been discussed in literature [39-42].

The aim of this simulation is to examine the affected magnetic source on nanofluid hydrothermal treatment in a square enclosure.MAC algorithm is chosen to employ the governing partial non-dimensional equations. The literature survey shows that, the investigation of convection and heat transfer of ferrofluid with base fluid in a square enclosure in presence external magnetic field and spatially varying magnetic wire has been wide range of Rayleigh number and Hartmann number to the best of authors' knowledge has not been studied so far. Effects of Rayleigh and Hartmann numbers, are taken into account to study heat transfer characteristics.

2. Mathematical modelling and Governing equations

A In this paper, the thermally active side walls of the cavity are maintained at uniform cold temperatures are considered while the bottom wall is maintained at high temperature and the other wall is thermally insulated. **Fig.1** reveals the current computational domain of interest with boundary conditions.

To express the magnetic field strength, one can consider that the magnetic source represents a magnetic wire placed vertical to the *x-y* plane at the point $\left(\overline{a},\overline{b}\right)$. The components of the magnetic field's intensity $\left(\overline{H_x},\overline{H_y}\right)$ and strength $\left(\overline{H}\right)$ can be considered as [45].

$$\overline{H_x}=\frac{\gamma}{2\pi}\frac{1}{\left(x-\overline{a}\right)^2+\left(y-\overline{b}\right)^2}\left(y-\overline{b}\right) \tag{1}$$

$$\overline{H_y}=\frac{\gamma}{2\pi}\frac{1}{\left(x-\overline{a}\right)^2+\left(y-\overline{b}\right)^2}\left(x-\overline{a}\right) \tag{2}$$

$$\overline{H}=\sqrt{\overline{H}_x^2+\overline{H}_y^2}=\frac{\gamma}{2\pi}\frac{1}{\sqrt{\left(x-\overline{a}\right)^2+\left(y-\overline{b}\right)^2}} \tag{3}$$

Where γ is the magnetic field's strength at the source (of the wire) and $\left(a,b\right)$ is the position where the source is located. Let us consider the unsteady two-dimensional natural convective laminar flow of fluid in a square cavity with length of side walls equal to *L*. The gravity acts normal to the *x*-axis and a magnetic source is considered by placing a magnetic wire vertically on to the *x y*-plane at the point $\left(a,b\right)$. In this study the magnetic source is located at e1, e2 and e3 (i.e. **e1**= (0.5 columns, 1.01 rows), **e2** = (0.5 columns, 1.01 rows) and **e3**= (0.5 columns, 1.01 rows)). The thermal Radiation and Joule heating are negligible. The thermo physical properties of the fluid are assumed to be constant except the density variation in the buoyancy force, which is approximated according to the Boussinesq approximation.

Under the above assumptions with the Boussinesq approximation, the governing equations of conservation of mass, momentum and energy equations can be written In the Cartesian coordinate system as follows:

$$\frac{\partial u}{\partial x}+\frac{\partial v}{\partial y}=0 \tag{4}$$

$$\frac{\partial u}{\partial t}+u\frac{\partial u}{\partial x}+v\frac{\partial u}{\partial y}=-\frac{1}{\rho_{nf}}\frac{\partial p}{\partial x}+\upsilon_{nf}\left(\frac{\partial^2 u}{\partial x^2}+\frac{\partial^2 u}{\partial y^2}\right) -\frac{\sigma_{nf}}{\rho_{nf}}\mu_0^2\left[\overline{H_y}^2u-\overline{H_x}\,\overline{H_y}v\right] \tag{5}$$

$$\frac{\partial v}{\partial t}+u\frac{\partial v}{\partial x}+v\frac{\partial v}{\partial y}=-\frac{1}{\rho_{nf}}\frac{\partial p}{\partial y}+\upsilon_{nf}\left(\frac{\partial^2 v}{\partial x^2}+\frac{\partial^2 v}{\partial y^2}\right) +\frac{\sigma_{nf}}{\rho_{nf}}\mu_0^2\left[\overline{H_x}\,\overline{H_y}u-\overline{H_x}^2v\right]+g\beta_{nf}\left(T-T_c\right) \tag{6}$$

$$\frac{\partial T}{\partial t}+u\frac{\partial T}{\partial x}+v\frac{\partial T}{\partial y}=\alpha_{nf}\left(\frac{\partial^2 T}{\partial x^2}+\frac{\partial^2 T}{\partial y^2}\right) +\frac{\sigma_{nf}}{\left(\rho c_p\right)_{nf}}\mu_0^2\left(\overline{H_y}u-\overline{H_x}v\right)^2 +\frac{\mu_{nf}}{\left(\rho c_p\right)_{nf}}\left\{2\left(\frac{\partial u}{\partial x}\right)^2+2\left(\frac{\partial v}{\partial y}\right)^2+\left(\frac{\partial v}{\partial x}+\frac{\partial u}{\partial y}\right)^2\right\} \tag{7}$$

Where $\mu_{nf}=\frac{1}{\left(1-\phi\right)^{2.5}}$

$$\rho_{nf}=\rho_s\phi+\left(1-\phi\right)\rho_f$$

$$\alpha_{nf}=\frac{\kappa_{nf}}{\left(\rho C_p\right)_{nf}}$$

$$\left(\rho C_p\right)_{nf}=\left(\rho C_p\right)_s\phi+\left(\rho C_p\right)_f\left(1-\phi\right)$$

$$\beta_{nf}=\beta_f\left(1-\phi\right)+\beta_s\phi$$

$$\frac{\kappa_{nf}}{\kappa_f}=\frac{-2\phi\left(\kappa_f-\kappa_s\right)+2\kappa_f+\kappa_s}{\phi\left(\kappa_f-\kappa_s\right)+2\kappa_f+\kappa_s}$$

$$\frac{\sigma_{nf}}{\sigma_f}=1+\frac{3\left(\frac{\sigma_s}{\sigma_f}-1\right)\phi}{\left(\frac{\sigma_s}{\sigma_f}+2\right)-\left(\frac{\sigma_s}{\sigma_f}-1\right)\phi}$$

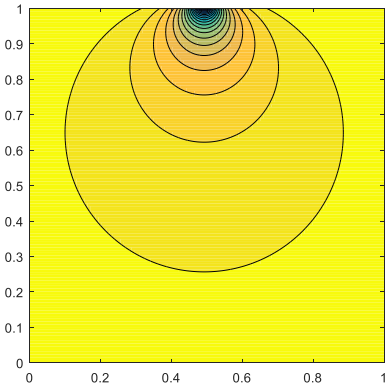

(a) *Hx (x,y)*

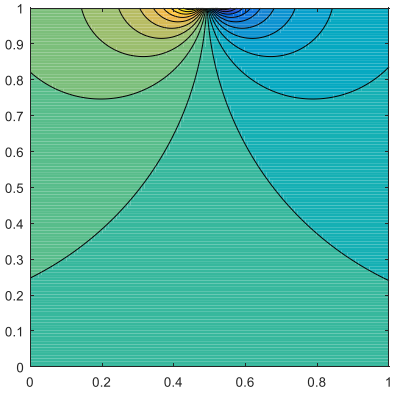

(b) *Hy (x,y)*

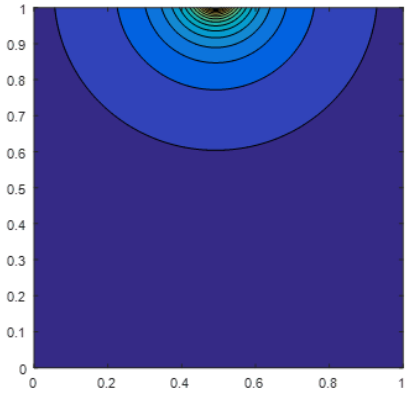

(c) *H (x,y)*

Figure. 1. *Contours of the (a) magnetic field intensity component in x direction Hx; (b) magnetic field intensity component in y direction Hy (c) magnetic field strength H.*

The following dimensionless variables are introduced:

$$\tau=\frac{t\upsilon}{L^2},X=\frac{x}{L},Y=\frac{y}{L},U=\frac{uL}{\upsilon},V=\frac{vL}{\upsilon}$$

$$\theta=\frac{T-T_c}{T_h-T_c},\ P=\frac{pL^2}{\rho\upsilon^2},\tag{8}$$

$$\left(H,H_x,H_y\right)=\frac{\left(\overline{H},\overline{H_x},\overline{H_y}\right)}{\overline{H_0}},\ \overline{H_0}=\overline{H}(a,0)=\frac{\gamma}{2\pi|b|}$$

Using (8), Equations (4) – (7) can be written in dimensionless form as

$$\frac{\partial U}{\partial X}+\frac{\partial V}{\partial Y}=0\tag{9}$$

$$\frac{\partial U}{\partial\tau}+U\frac{\partial U}{\partial X}+V\frac{\partial U}{\partial Y}=-\frac{\partial P}{\partial X}$$
$$+A\Pr\left(\frac{\partial^2U}{\partial X^2}+\frac{\partial^2U}{\partial Y^2}\right)-B\delta\left[H_y{}^2U-H_xH_yV\right]\tag{10}$$

$$\frac{\partial V}{\partial\tau}+U\frac{\partial V}{\partial X}+V\frac{\partial V}{\partial Y}=-\frac{\partial P}{\partial Y}$$
$$+C\Pr\left(\frac{\partial^2V}{\partial X^2}+\frac{\partial^2V}{\partial Y^2}\right)-D\delta\left[H_x{}^2V-H_xH_yU\right]+E\chi\theta\tag{11}$$

$$\frac{\partial\theta}{\partial\tau}+U\frac{\partial\theta}{\partial X}+V\frac{\partial\theta}{\partial Y}=F\left(\frac{\partial^2\theta}{\partial X^2}+\frac{\partial^2\theta}{\partial Y^2}\right)$$
$$+G\lambda\left(H_yU-H_xV\right)^2\tag{12}$$
$$+H\times Ec\left\{2\left(\frac{\partial U}{\partial X}\right)^2+2\left(\frac{\partial V}{\partial Y}\right)^2+\left(\frac{\partial V}{\partial X}+\frac{\partial U}{\partial Y}\right)^2\right\}$$

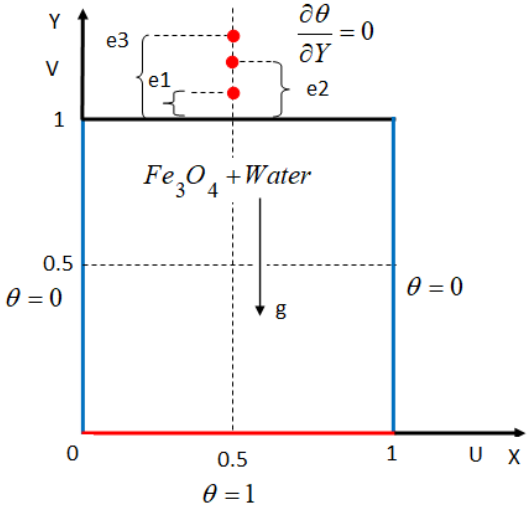

Figure. 2. Physical geometry

With dimensionless parameters

$$Ha=L\mu_0H_0\sqrt{\frac{\sigma}{\mu}},\ Ec=\frac{\upsilon^2}{c_p\Delta TL^2},\ \Pr=\frac{\upsilon}{\alpha},\ \chi=Ra\times\Pr,$$

$$Ra=\frac{g\beta\left(T-T_c\right)L^3}{\upsilon\alpha},\delta=Ha^2\times\Pr\ \lambda=Ha^2\times Ec,$$

$$A=\frac{\mu_{nf}/\mu_f}{\rho_{nf}/\rho_f}=C,\ B=\frac{\sigma_{nf}/\sigma_f}{\rho_{nf}/\rho_f}=D,\ E=\frac{\beta_{nf}}{\beta_f},$$

$$F=\frac{\kappa_{nf}/\kappa_f}{\left(\rho C_p\right)_{nf}/\left(\rho C_p\right)_f},\ G=\frac{\sigma_{nf}/\sigma_f}{\left(\rho C_p\right)_{nf}/\left(\rho C_p\right)_f},$$

$$H=\frac{\mu_{nf}/\mu_f}{\left(\rho C_p\right)_{nf}/\left(\rho C_p\right)_f}$$

The appropriate boundary conditions for the present problem are
On the bottom wall $\theta = 1$
On the side walls $\theta = 0$
On the top wall $\frac{\partial \theta}{\partial n} = 0$
On all walls $U = V = 0$
The local Nusselt number on the heat source surface can be expressed as

$$Nu = \frac{\kappa_{nf}}{\kappa_f} \frac{\partial \theta}{\partial X}\bigg|_{Y=0}$$

The average Nusselt number is evaluated by integrating *Nu* along the heat source

$$\overline{Nu} = \frac{1}{L}\int_0^L Nu\, dX$$

Flow field of fluid in the present problem is visualized through streamline which is obtained from stream function. Stream function is defined from velocity components *U* and *V*. The two-dimensional flow stream function and velocity components Relationsare given by,

$$U = \frac{\partial \psi}{\partial Y},\ V = -\frac{\partial \psi}{\partial X}$$

Table 1. Thermo physical properties of water and nanoparticles

	$\rho\left(kg/m^3\right)$	$C_p\left(J/kg\ k\right)$	$\kappa(W/mk)$	$\beta\times10^5\left(k^{-1}\right)$	$\sigma\left(\Omega^{-1}m^{-1}\right)$
Water	997.1	4179	0.613	21	0.05
Fe_3O_4	5200	670	6	1.3	25,000

3. Computational details

3.1. Numerical procedure

The MAC Algorithm has been adopted for the solution of the present specified problem. The coupled highly nonlinear governing equations were converted into weak conservative form in the first step. The staged grid system is used for solving Navier Stokes equation while the central difference scheme is used to solve energy equation. We integrate in time by an incremental step $d\tau$ in each iteration, until the final time 1.0 is reached. Iterative technique is used to solve the resulting equations. The solution process was sustained until the required convergent criterion was full-filled which was $\sum_{i,j}\left|\Omega_{i,j}^{k+1} - \Omega_{i,j}^{k}\right| < 10^{-6}$, the generic variable Ω stands for U, V, P, θ and *k* denotes the iteration time levels. In the above inequality the subscripts *i, j* represents the space coordinates *X* and *Y* respectively.

3.2. Code validation

A code validation is performed for checking the reliability of the present code. The present code is compared with the results of D. C. Wan *et al.* [23]. The streamlines and isotherms are compared for $Ra = 10^4$ and $\Pr = 0.7$ as shown in **Fig. 3.** From the figure it is evident that the streamlines and isotherms produced by the present code are matched with previously published work by D. C. Wan *et al.* [44]. Also, the Local Nusselt number of hot walls is compared for different values of *Gr* as shown in **Fig.4.** The error is very negligible if the Nusselt number is compared. The comparisons reveal an excellent agreement with the reported studies, and hence the present numerical code is completely reliable.

4. Results and discussions

In this computational study the effect of magnetic wire positions on controlling of magnetohydrodynamics natural convection heat transfer in an enclosure which is heated by uniformly along the bottom wall, cold vertical walls and adiabatic top wall is examined. MAC algorithm is adapted to obtained numerical solution. The square cavity is filled with Fe_3O_4– Water nanofluid (with detail thermal properties of Table. 1). The active key parameters effects such as: Rayleigh number ($Ra=10^3$, 10^4 and 10^5), Hartmann number (Ha=0-5) with $Ec=10^{-5}$ and volume fraction of nanoparticles ($\phi = 0 - 0.02$) on fluid flow and heat transfer are investigated when Pr=6.8.

The influence of magnetic wire position and Rayleigh number on isotherms and streamlines are presented in **Figs.5-8**. It is reveals from these computational Figs. that the flow cells enhance as the magnetic wire place increases from e1 to e3. Also, it can be observed that the temperature contours move upward. The temperature contours are away from bottom wall when increasing of *Ra*. In addition, that, by enhancing of Rayleigh number the heat transfer mechanism is shifted from conduction to convection. When the magnetic field is applied on the cavity, the velocity profiles are suppressed owing to the retarding influence of the Lorenz force. Thus, augmentation of convection is suppressed significantly. The core vortex cell is moves downwards vertically when the magnetic wire is varying to e3 to e1 positions. The thermal plume intensity is enhanced when increasing of Rayleigh number and magnetic wire position. For this reason, the cluster temperature contours are formed along the cold walls.

The effect of magnetic wire (0.5, 1.05) on velocity profiles for $Ra=10^5$, Ha=5, $\phi = 0.02$ are presented in the **Fig.9**. Flow behavior within the enclosure is described various sections of the cavity. The U-velocity (**Fig.9**a) along the vertical line from at X=0.1 to X=0.4 is gradually increased and fall down to at X=0.5 and the symmetric nature and opposite velocity is exhibited from X=0.6 to X=0.9. The V-velocity (**Fig.9**b) along the horizontal line from Y=0.1 to Y=0.9 is reveals that the increasing nature is shown from Y=0.1 to Y=0.5 and decreasing function from Y=0.5 to Y=0.9. In the middle of the enclosure, the velocity is more compare to other positions, due to the uniform heating of bottom wall the fluid rise up in middle part and fall down to cold walls.

The impact of magnetic wire (0.5, 1.05) on velocity profiles for $Ra=10^5$, Ha=5, $\phi = 0.02$ are shown in the **Fig.10**. Fluid flow velocity variations within the enclosure are presented different sections of the cavity. The U-velocity (**Fig.10**a) along the vertical line from at X=0.1 to X=0.4 is gradually increased and at X=0.5 the fluid velocity is constant up to Y=0.8 while the fluid velocity raises and decreases to zero. The symmetric nature and opposite velocity are exhibited from X=0.6 to X=0.9. The V-velocity (**Fig.10**b) along the horizontal line from Y=0.1 to Y=0.9 is reveals that the increasing profile of V is shown from Y=0.1 to Y=0.5 and decreasing profile of V from Y=0.5 to Y=0.9. In the middle of the enclosure, the velocity is more compare while this higher velocity place at X=0.5 shifted to X=0.4 near the magnetic wire, due to the higher impact of magnetic strength.

The variations of local Nusselt number by the impact of magnetic wire positions, Hartmann number and Rayleigh number are illustrating the **Figs.11-13** for fixed $\phi = 0.02$. The heat enhancement is controlled by varying of magnetic wire is presented in **Fig.11.** The magnetic wire is varying from e1 to e5

for Ra=10^5, Ha=5, $\phi = 0.02$ which leads to increasing the local Nusselt number. The temperature distribution bottom wall is symmetric about X=0.5, higher temperature is observed at ends of the hot wall and minimum at middle of the bottom wall. When we expect, the heat transfer rate is reduced with increasing of Hartmann number Ha for Ra=10^5, $\phi = 0.02$, positions of Magnetic wire (0.5,1.01). the clear pictorial representation is seen in **Fig.12.** The local Nusselt number gradually increased when increasing of Rayleigh number with Ha=5, $\phi = 0.02$ due to the buoyancy effect is enhanced then gradually increasing of fluid flow velocity (it is observed in **Fig.13)**.

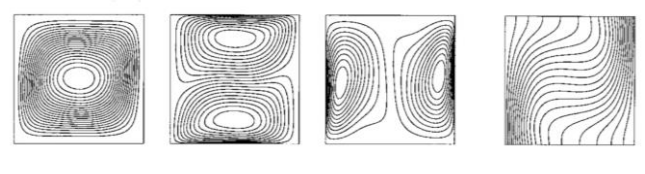

(a)

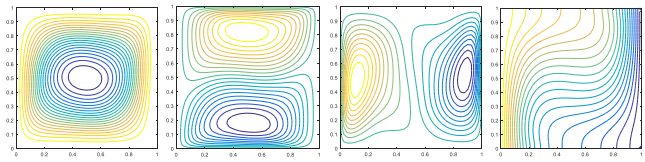

(b)

Figure. 3. Code validation study, comparison of streamlines *u*-velocity, *v*-velocity and isotherms with D. C. Wan *et al.* [15] $Ra = 10^4$ *and* $\Pr = 0.7$. (a) D. C. Wan *et al.* [44], (b) Present solver (MAC)

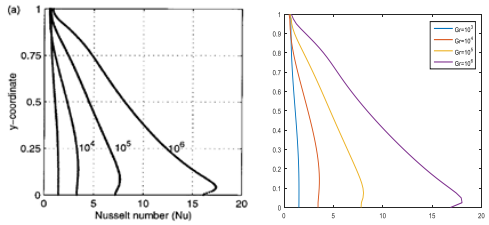

(a) (b)

Figure. 4. Comparison ofLocalNusselt number variation of hot wall for $10^3<Gr<10^6$(a) D. C. Wan *et al.* [44], (b) Present solver (MAC)

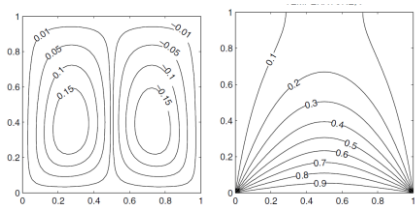

Pr=0.71

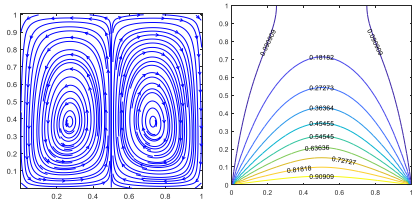

Pr=0.7, Ec=0 Ha=0, $\phi = 0$

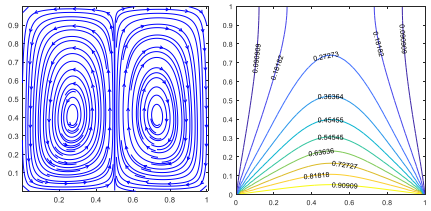

Pr=6.8, Ec=0 Ha=0, $\phi = 0$

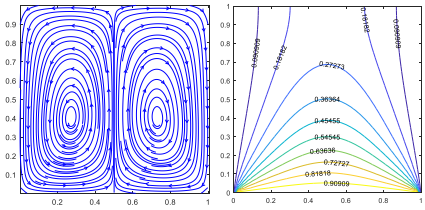

Pr=6.8, Ec=10^{-5} Ha=0, $\phi = 0.02$

Figure. 5. Streamlines and isotherms for bottom wall heating with Ra=10^3 and various values of Prandtl number, top row results of Basak*et al*. [43] and bottom row results are nanofluid

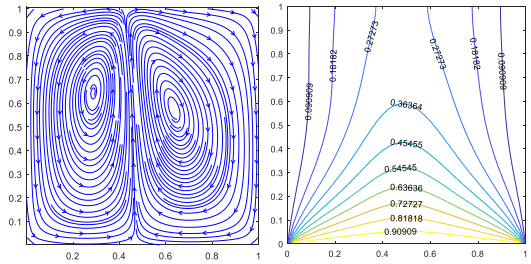

$e1 = 1.01$

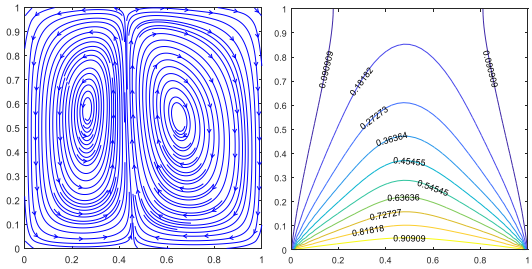

$e2 = 1.02$

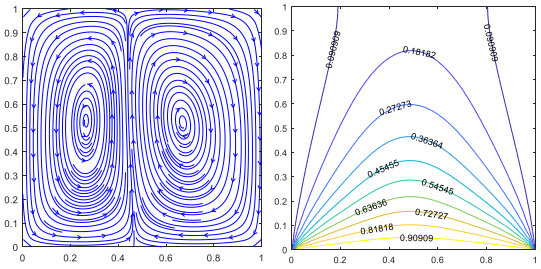

$e3 = 1.03$

Figure. 6. The effect of magnetic wire positions on streamlines (left) and isotherms (right) when Ra=10^3, Ha=5, $\phi = 0.02$

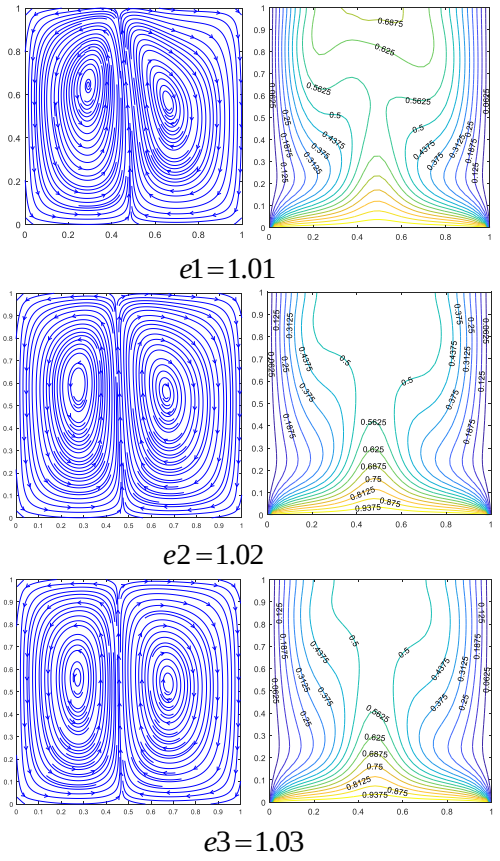

$e1 = 1.01$

$e2 = 1.02$

$e3 = 1.03$

Figure. 7. The effect of magnetic wire positions on streamlines (left) and isotherms (right) when Ra=10^4, Ha=5, $\phi = 0.02$

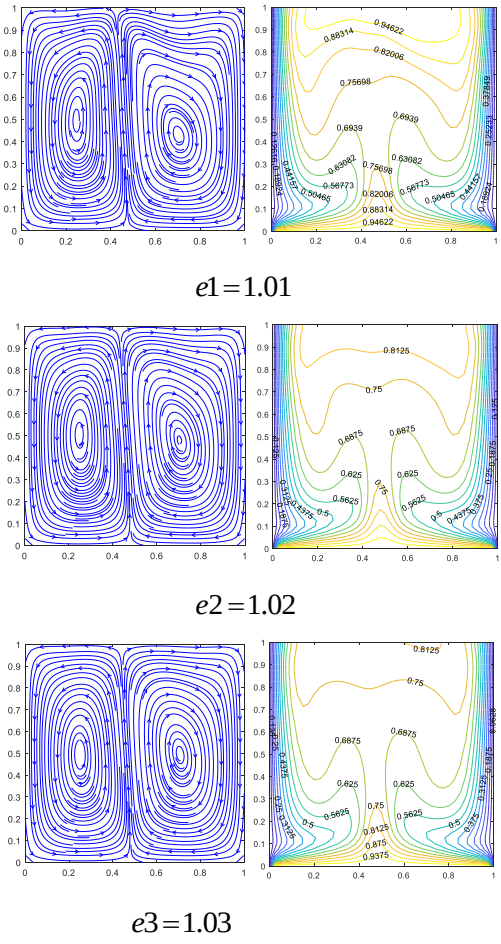

$e1 = 1.01$

$e2 = 1.02$

$e3 = 1.03$

Figure. 8. The effect of magnetic wire positions on streamlines (left) and isotherms (right) when Ra=10^5, Ha=5, $\phi = 0.02$

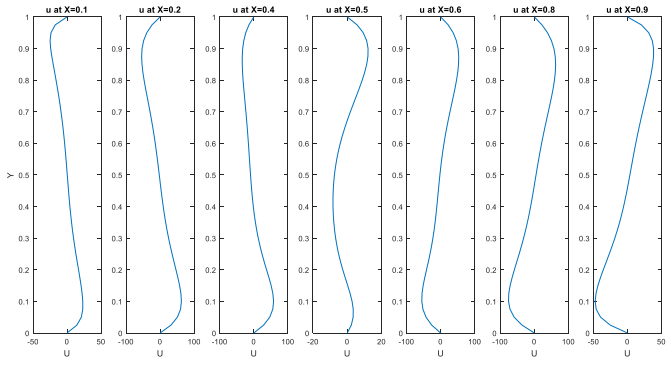

(a)

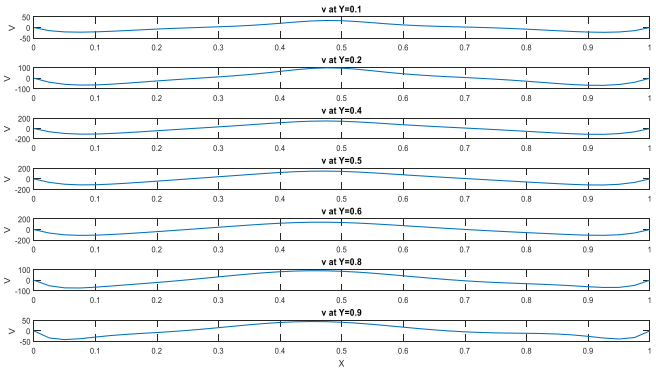

(b)

Figure. 9. The velocity profile U-(a), V-(b) for various section with Ra=10^5, Ha=5, $\phi = 0.02$ and magnetic wire position (0.5, 1.05).

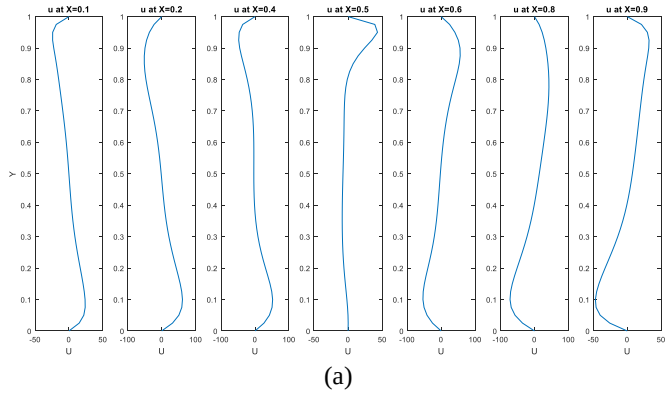

(a)

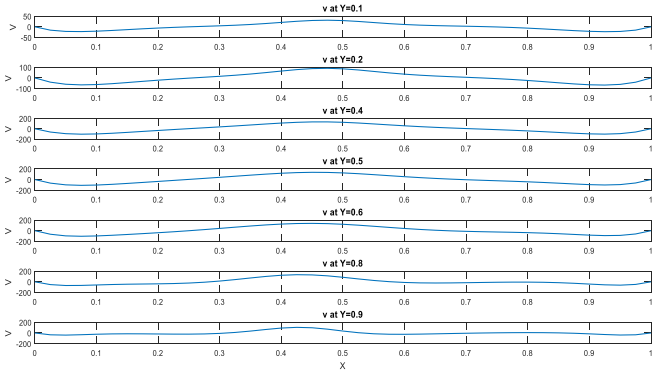

(b)

Figure. 10. Velocity profile U-(a), V-(b) for various section with Ra=10^5, Ha=5, $\phi = 0.02$ and magnetic wire position (0.5, 1.01)

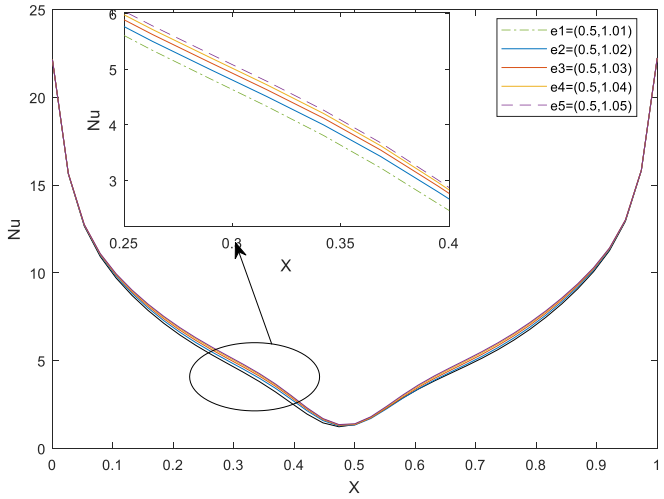

Figure. 11. Local Nusselt number along the hot wall with Ra=10^5, Ha=5, $\phi = 0.02$ and various positions of Magnetic wire.

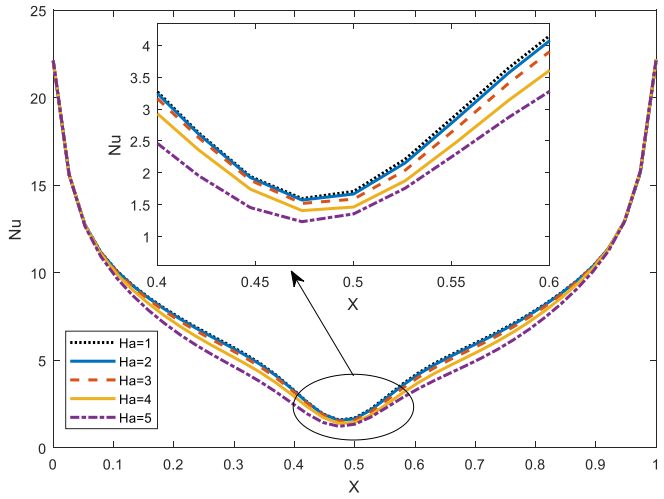

Figure. 12. Local Nusselt number along the hot wall with Ra=10^5, $\phi = 0.02$, positions of Magnetic wire (0.5,1.01) and various values of Ha.

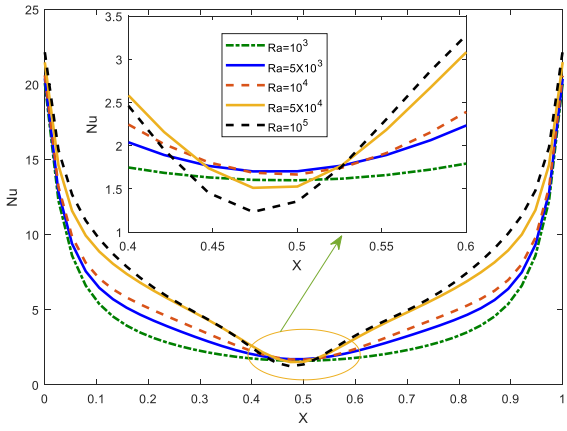

Figure. 13. Local Nusselt number along the hot wall with Ha=5, $\phi = 0.02$, positions of Magnetic wire (0.5,1.01) and various values of Ra.

5. Conclusions

In this paper the impact of magnetic wire on nanofluid (Fe_3O_4-water) flow in an enclosure with isothermal temperature boundary conditions and adiabatic to wall has been studied with MAC algorithm. This numerical analysis is performed for pertinent key parameters in the following ranges: Rayleigh number 10^3-10^5, Hartmann number 0-5, the volume fraction is $\phi = 0.02$ and the fixed Prandtl number 6.8 where the positions of magnetic wire is from e1-e5. The study was carried out for various mentioned governing parameters and the results indicates that, Augmentation of heat transfer reduces with an increasing of Hartman number while at the same time heat transfer is increases when increasing of magnetic wire positions. The increase in Hartmann number reduces the both the velocity profiles (*U* and *V* components). The increase in Rayleigh number and magnetic wire positions which leads to enhance the local Nusselt number then it is a deceasing function of *Ha*.

Nomenclature

C_P	Specific heat cavity
B	Constant applied Magnetic field
$\overline{H_X}$	Magnetic field Intensity in X-direction
$\overline{H_Y}$	Magnetic field Intensity in Y-direction
$\overline{H}$	Magnetic field strength
L	Length of the cavity
K	Thermal conductivity, (W m^{-1} k^{-1})
T	Temperature, (K)
u,v	Velocity components ,(m s^{-1})
U,V	Dimensionless velocity components
X,Y	Dimensionless Cartesian co-ordinates,(m)
Ec	Eckert Number
Gr	Grashof number
Pr	Prandtl Number
Ha	Hartmann number
Nu	Nusselt number
Ra	Rayleigh Number

Greek Symbols

λ	Thermal relaxation parameter
τ	Dimensionless time
g	Gravitational acceleration
ψ	Stream function
η	Efficiency
ϕ	Nano particle volume fraction
ρ	Fluid density,(kg m^{-3})
α	Thermal Diffusivity,(m^2 s^{-1})
β	Thermal Expansion co-efficient
υ	Kinematic Viscosity
σ	Electrical conductivity function

Sub Scripts

nf	Nano Fluid
f	Base Fluid
s	Solid Particle

References

[1] R.E. Rosenzweig, Ferrohydrodynamics, Dover Publications, Mineola, New York, 1997.

[2] S. Odenbach, Colloidal Magnetic Fluids: Basics Development and Application of Ferrofluids, Springer, Berlin, Heidelberg, 2009.

[3] M. Abareshi, E.K. Goharshadi, S. MojtabaZebarjad, H. KhandanFadafan, A. Youssefi, Fabrication, characterization and measurement of thermal conductivity of Fe3O4 nanofluids, J. Magn. Magn. Mater. 322 (2010) 3895– 3901.

[4] Y. Mitamura, S. Arioka, D. Sakota, K. Sekine, M. Azegami, Application of a magnetic fluid seal to rotary blood pumps, J. Phys.-Condens. Mater. 20 (2008) 204145.

[5] I. Nkurikiyimfura, Y. Wang, Z. Pan, Heat transfer enhancement by magnetic nanofluids - a review, Renewable Sustainable Energy Rev. 21 (2013) 548–561.

[6] D. Baranwal, T.S. Deshmukh, MR-fluid technology and its application-a review, Int. J.Emerging Technol. Adv. Eng. 2 (2012) 563–569.

[7] H. Yamaguchi, I. Kobori, Y. Uehata, K. Shimada, Natural convection of magnetic fluid in a rectangular box, J. Magn. Magn. Mater. 20 (1999) 264–267.

[8] H. Yamaguchi, Z. Zhang, S. Shuchi, K. Shimada, Heat transfer characteristics of magnetic fluid in a partitioned rectangular box, J. Magn. Magn. Mater. 252 (2002) 203–205.

[9] T.P. Bednarz, C. Lei, J.C. Patterson, H. Ozoe, Effects of atransverse orizontal magnetic field on natural convection of a paramagnetic fluid in a cube, Int. J. Therm. Sci. 48 (2009) 26–33.

[10] Q. Li, Y. Xuan, Experimental investigation on heat transfer characteristics of magnetic fluid flow around a fine wire under the influence of an external magnetic field, Exp. Therm. Fluid Sci. 33 (2009) 591–596.

[11] A.N. Afifah, S. Syahrullail, N.A. Che Sidik, Natural convection of alumina-distilled water nanofluid in cylindrical enclosure: an experimental study, J. Adv. Res. FluidMech. Therm. Sci. 12 (1) (2015) 1–10.

[12] B. M'hamed, N.A. Sidik, M.F. Akhbar, R. Mamat, G. Najafi, Experimental study on thermal performance of MWCNT nanocoolant in PeroduaKelisa 1000 cc radiator system, Int. Communication Heat Mass Transf. 24 (May 2016).

[13] N.A. Che Sidik, O.A. Alawi, Computational investigations on heat transfer enhancement using nanorefrigerants, J. Adv. Res. Des. 1 (2014) 35–41.

[14] M.A. Khattak, A. Mukhtar, S. Kamran Afaq, Application of nano-fluids as coolant in heat exchangers: a review, J. Adv. Rev. Sci. Res. 22 (1) (2016) 1–11.

[15] C.S. Nor Azwadi, I.M. Adamu, M.M. Jamil, Preparation methods and thermal performance of hybrid nanofluids, J. Adv. Rev. Sci. Res. 24 (1) (2016) 13–23.

[16] C.K. Sinz, H.E. Woei, M.N. Khalis, S.I. Ali Abbas, Numerical study on turbulent force convective heat transfer of hybrid nanofluid, Ag/HEG in a circular channel with constant heat flux. (2016), J. Adv. Res. Fluid Mech. Therm. Sci. 24 (2016) 1–11.

[17] D.G. Jehad, G.A. Hashim, Numerical prediction of forced convective heat transfer and friction factor of turbulent nanofluid flow through straight channels, J. Adv. Res. Fluid Mech. Therm. Sci. 1 (2014) 1–10.

[18] Y.K. Lee, The use of nanofluids in domestic water heat exchanger, J. Adv. Res. Appl. Mech. 3 (2014) 9–24.

[19] S.B. Abubakar, N.A. Che Sidik, Numerical prediction of laminar nanofluid flow in rectangular microchannel heat sink, J. Adv. Res. Fluid Mech. Therm. Sci. 7 (2015) 29–38.

[20] Khanafer K, Vafai K, Lightstone M. Buoyancy-driven heat transfer enhancement in a two-dimensional enclosure utilizing nanofluids. International Journal of Heat and Mass Transfer 2003; 46: 3639–53.

[21] Jang SP, Choi SUS. Free convection in a rectangular cavity (Benard convection) with nanofluids, Proceedings of IMECE04. Anaheim, California, USA; 2004. pp. 1–7.

[22] Floriana D. Stoian and Sorin Holotescu, experimental study of natural convection enhancement using a Fe_3O_4-water based magnetic nanofluid, journal of Nanoscience and Nanotechnology, 12 (2012) 8211-8214.

[23] Gul A, Khan I, Shafie S, Khalid A, Khan A (2015) Heat Transfer in MHD Mixed Convection Flow of a Ferrofluid along a Vertical Channel. PLoS ONE 10(11): e0141213.

[24] Nader Ben-Cheikh, Ali J. Chamkha, Brahim Ben-Beya, Taieb Lili, Natural convection of water - Based nanofluid in a square enclosure with non-uniform heating of bottom wall, Journal of Modern Physics, 2013, 4, 147-159.

[25] Omid Ghaffarpasand, Numerical study of MHD natural convection inside a sinusoidally heated lid-driven cavity filled with Fe_3O_4 -water nanofluid in the presence of Joule heating, Applied Mathematical Modelling 40 (2016) 9165–9182.

[26] Neshat Rahimpour, Mostafa Keshavarz Moraveji, Free convection of water–Fe3O4 nanofluid in an inclined cavity subjected to a magnetic field: CFD modeling, sensitivity analysis, Advanced Powder Technology 28 (2017) 1573–1584.

[27] A. Abedini, T. Armaghani, Ali J. Chamkha, MHD free convection heat transfer of a water– Fe3O4 nanofluid in a baffled C-shaped enclosure, Journal of Thermal Analysis and Calorimetry, (2019) 135: 685-695.

[28] Keshavarz Moraveji, M,Hejazian M., Natural convection in a rectangular enclosure containing an oval-shaped heat source and filled with Fe3O4/water nanofluid. Int. Commun. Heat Mass Transf., 2013; 44:135–46.

[29] Rosensweig RE., Ferrohydrodynamics., London: Cambridge University Press; 1985.

[30] Hiegeister R, Andra W, Buske N, Hergt R, Hilger I, Richter U, et al. Application of magnetite ferrofluids for hyperthermia. J MagnMagn Mater 1999; 201:420–2.

[31] Nakatsuka K, Jeyadevan B, Neveu S, Koganezawa H. The magnetic fluid for heat transfer applications. J MagnMagn Mater 2002; 252:360–2.

[32] Shuchi S, Sakatani K, Yamaguchi H. An application of a binary mixture of magnetic fluid for heat transport devices. J MagnMagn Mater 2005; 289:257– 9.

[33] M. Sheikholeslami, D.D. Ganji, Free convection of Fe3O4-water nanofluid under the influence of an external magnetic source, J. Mol. Liq. 229 (2017) 530–540.

[34] M. Sheikholeslami, K. Vajravelu, Nanofluid flow and heat transfer in a cavity with variable magnetic field, Appl. Math. Comput. 298 (2017) 272–282.

[35] Mohsen Sheikholeslami, DavoodDomiriGanji, Numerical investigation of nanofluid transportation in a curved cavity in existence of magnetic source,Chem. Phys. Lett. 667 (2017) 307–316.

[36] M. Sheikholeslami, Numerical simulation of magnetic nanofluid natural convection in porous media, Phys. Lett. A 381 (2017) 494–503.

[37] Kandelousi M. Sheikholeslami, Effect of spatially variable magnetic field on ferrofluid flow and heat transfer considering constant heat flux boundary condition, Euro. Phys. J. Plus (2014) 129–248.

[38] M. Sheikholeslami, M.M. Rashidi, Effect of space dependent magnetic field on free convection of Fe3O4-water nanofluid, J. Taiw. Inst. Chem. Eng. 56 (2015) 6–15.

[39] K.Venkatadri, S. GouseMohiddin and M. Suryanarayana Reddy, Numerical Analysis of Unsteady MHD Mixed Convection Flow in a Lid-Driven Square Cavity with Central Heating on Left Vertical Wall, Applications of Fluid Dynamics, Lecture Notes in Mechanical Engineering, Chapter 26 (2018) 355-370.

[40] B MD Hidayathulla Khan, K Venkatadri, O. Anwar Be´g, V.Ramachandra Prasad, B. Mallikarjuna. " Natural Convection in a Square Cavity with Uniformly Heated and/or Insulated Walls Using Marker-and-Cell Method" International Journal of Applied and Computational Mathematics, 4 (2018) 61.

[41] Venkatadri K, GouseMohiddin S, Suryanarayana Reddy M., Hydromagneto quadratic natural convection on a lid-driven square cavity with isothermal and a non-isothermal bottom wall, Engineering Computations, 34 (8) (2017) 2463-2478.

[42] K.Venkatadri, S. GouseMohiddin, M. Suryanarayana Reddy, Mathematical modeling of unsteady MHD double-diffusive natural convection flow in a square cavity, Frontiers in Heat and Mass Transfer, 9 (2017) No.33.

[43] Tanmay Basak, S. Roy, A.R. Balakrishnan, Effects of thermal boundary conditions on natural convection flows within a square cavity, International Journal of Heat and Mass Transfer 49 (2006) 4525–4535.

[44] D. C. Wan, B. S. V. Patnaik, and G. W. Wei, A new benchmark quality solution for the buoyancy-driven cavity by discrete singular convolution, *Numerical Heat Transfer, Part B*, 2001,40, 199- 228.

[45] M. Hatami, J. Zhou, J. Geng, D. Jing, Variable magnetic field (VMF) effect on the heat transfer of a half-annulus cavity filled by Fe_3O_4-Water nanofluid under the constant heat flux, journal of Magnetism and Magnetic Materials, 451 (2018) 173-182.